Large eddy simulations of flow instabilities in a stirred tank generate by a Rushton turbine

Fan, Jianhua; Wang, Yundong; Fei, Weiyang

Published in:
Chinese Journal of Chemical Engineering

Publication date:
2007

Large eddy simulations of flow instabilities in a stirred tank generated by a Rushton turbine*

FAN Jianhua (樊建华)[a,b], WANG Yundong (王运东)[a **], FEI Weiyang (费维扬)[a]

[a] The State Key Laboratory of Chemical Engineering, Department of Chemical Engineering, Tsinghua University, Beijing 100084, China

[b] Department of Civil Engineering, Technical University of Denmark, Building 118, Brovej, DK-2800 Kgs. Lyngby, Denmark

Abstract The aim of this work is to investigate the flow instabilities in a baffled, stirred tank generated by a single Rushton turbine by means of large eddy simulation (LES). The sliding mesh method was used for the coupling between the rotating and the stationary frame of references. The calculations were carried out on the "Shengcao-21C" supercomputer using a computational fluid dynamics (CFD) code CFX5. The flow fields predicted by the LES simulation and the simulation using standard k-ε model were compared to the results from particle image velocimetry (PIV) measurements. It is shown that the CFD simulations using the LES approach and the standard k-ε model agree well with the PIV measurements. Fluctuations of the radial and axial velocity are predicted at different frequencies by the LES simulation. Velocity fluctuations of high frequencies are seen in the impeller region, while low frequencies velocity fluctuations are observed in the bulk flow. A low frequency velocity fluctuation with a nondimensional frequency of 0.027 Hz is predicted by the LES simulation, which agrees with experimental investigations in the literature. Flow circulation patterns predicted by the LES simulation are asymmetric, stochastic and complex, spanning a large portion of the tanks and varying with time, while circulation patterns calculated by the simulation using the standard k-ε model are symmetric. The results of the present work give better understanding to the flow instabilities in the mechanically agitated tank. However, further analysis of the LES calculated velocity series by means of fast Fourier transform (FFT) and/or spectra analysis are recommended in future work in order to gain more knowledge of the complicated flow phenomena.

Keywords: stirred tank, flow instabilities, computational fluid dynamics (CFD), large eddy simulation (LES), k-ε model, particle image velocimetry (PIV)

1 INTRODUCTION

Mechanically agitated tanks are widely used in chemical and allied industries. Fluid flow in such tanks is in many cases highly three dimensional, complex and stochastic with vortical structures at different scales. Therefore, knowledge of the flow structures are of great importance for the understanding of the mixing processes in stirred tanks.

There have been numerous investigations of the fluid flow in stirred tanks since 1960's. These studies can be divided into two categories: experimental investigations and numerical simulations. Experimentally, flow visualization techniques such as laser Doppler velocimetry (LDV), particle image velocimetry (PIV) were used to measure the velocity fields in stirred tanks. Most of the studies in the 1980's were the flow field measurements obtained by averaging the instantaneous flow fields over 360 degree of the impeller revolution[1,2]. Later in the 1990's, several attempts were made to measure angle-resolved flow characteristics in stirred tanks. By means of LDV, Schaefer et al.[3], Lee and Yianneskis[4] measured turbulence

* Received 2006-xx-xx, accepted 2006-09-17.

** To whom correspondence should be addresses. E-mail: wangyd@tsinghua.edu.cn.

properties of the impeller stream induced by a RT impeller. Comprehensive data of high spatial resolution were obtained through angle-resolved and time-resolved LDV measurement.

LDV is essentially a single point velocity measurement technique. Instantaneous measurement of flow structure is therefore impossible. To capture the instantaneous flow structures in stirred tanks, PIV measurement is necessary. Ranade et al.[5] studied the trailing vortices behind the blades of a Rushton turbine by PIV measurement. Both angle-resolved and angle-averaged flow fields near the impeller blades were obtained. Using the same technique, Sharp and Adrian[6] studied the instantaneous flow structures in a region surrounding the blade tip of a Rushton turbine mixer.

The investigations of flow structures are complicated by the presence of flow macro-instability (MI) in stirred tanks. Extensive investigations have clearly shown the existence of MI as large-scale, low-frequency flow pattern alterations. Myers et al.[7] used PIV technique to study instabilities in the flow fields produced by a pitch blade turbine (PBT) and by a high efficiency impeller. Transients among different flow patterns with time scales corresponding to 40-300 impeller revolutions were observed via power spectral density (PSD) analysis of time series of spatially averaged vorticity. Montes et al.[8] investigated flow macro-instabilities in a stirred reactor equipped with a six bladed 45º PBT, using a combination of LDV measurement, flow visualization, spectral analysis and wavelet transform. Hasal et al.[9] implemented the proper orthogonal decomposition (POD) technique to analyze MI. The proposed analysis method was successfully applied at both low and moderate Reynolds number. Roussinova et al.[10] studied MI in the impeller stream and in the upper corner of the stirred vessel with four commonly used impellers by means of a velocity decomposition technique. The intensity of the MI and its influence on root mean square (RMS) velocity measurements were quantified and the investigations covered a wide range of impellers and geometries. Recently there appear several attempts in the literature trying to explain the mechanism of MI[11-14].

Correspondingly, CFD simulation of fluid flow in stirred tanks, from Reynolds-averaged Navier-Stokes (RANS) approach, large eddy simulation (LES) to direct numerical simulation (DNS), experienced a similar development process: from simplicity to complexity. Since 1980's, reports on CFD investigations of fluid flow in stirred tanks have been flourishing. Most of the investigations solve the Reynolds-averaged Navier-Stokes (RANS) equations in combination with a closure model for the Reynolds stresses[15-26]. In many of these simulations, the coupling between the rotating impeller and the stationary tank was solved by the sliding mesh method, in which the geometry of the individual blades was modeled using a grid rotating with the impeller, while the bulk flow was calculated in a stationary frame. Sun et al.[25] and Fan et al.[26] addressed the coupling problem with an inner-outer iterative procedure in their simulations of turbulent and laminar flow in a stirred tank with a Rushton turbine. As an alternative way to model the relative motion between the tank and the impeller, Min et al.[27] used the multi-reference frame (MRF) method to calculate the fluid flow in a

stirred tank with multiple hydrofoil impellers. In these simulations, part of the unsteadiness and flow periodicity due to impeller revolution were considered. The presence and the substantial mean velocity and RMS fluctuations associated with MI in stirred tanks were, however, not taken into account. Therefore, RANS methods offer only an approximation to the mixing processes involved. Consequently, LES or DNS are necessary to capture such instabilities.

DNS provides the most exact approach in which the mechanism involved in turbulent mixing can be accurately presented. DNS resolves all turbulent lengths and time scales by directly integrating the Navier-Stokes equations using a very fine grid, which makes the approach prohibitively expensive even with the most powerful computers of the present day. Bartels et al.[28] have attempted a DNS simulation of a stirred tank operating at Re= 7300 using a sliding mesh technique. To reduce the computational cost, twofold periodicity of the solution domain was assumed and the finite thickness of the blades and disk was not taken into account. However, as the resolution of all length and time scales in the flow would require enormous amount of cells and time steps, DNS is not practical for research and engineering purpose at present.

Recently, the large eddy simulation (LES) approach has been used as a compromise between the extremes of DNS and RANS. Eggels[29] and Derksen and van den Akker[30, 31] carried out LES simulations of fluid flow in a baffled stirred tank reactor using the lattice–Boltzmann scheme. To solve the problem of relative motion between the rotating impeller and the stationary baffles, adaptive force-field procedure was used to describe the action of impeller on the flow. The lattice-Boltzmann method solves a simplified kinetic model that is only an approximation of the complete Navier-Stokes equation. The advantage is that the computations to be performed are significantly reduced compared with that for the full equations, thus allowing for very fine grids and long simulation and averaging times. However, this approach may have disadvantages for some tanks if the smallest scale of the system is smaller than the diameter of the impeller, and the later, in turn, is smaller than the overall size of the tank. Revstedt et al.[32] presented results of LES simulation of a baffled tank stirred by a Ruston turbine. The filtered Navier-Stokes equations were discretized on a system of locally refined Cartesian grids and were solved using finite difference method. The subgrid-scale stresses, not explicitly modeled in their investigations, were thought to be included in the calculation by the numerical dissipation association with the truncation errors of finite difference schemes. Using CFD code FLUENT 5, Bakker et al.[33] examined a tank with 45° PBT (D/T=0.35, C/T=0.46, T=0.292 m) by means of LES simulation. The simulation was verified with PIV snapshots reported by Myers et al.[8]. A similar PBT tank with the diameter of 0.24 m was investigated by Roussinova et al.[12]. LES simulation was claimed to be able to successfully predict the frequency of the flow macro-instabilities in the stirred tank. Alcamo et al.[34] investigated the turbulent flow generated in an unbaffled stirred tank by means of LES simulation. The numerical predictions were compared to the literature results with comparable configurations and to PIV measurements. A very good agreement was

shown for both time-averaged resolved fields and turbulence quantities. The credibility of LES and RANS approaches for the prediction of fluid flow in stirred tanks was evaluated by Hartmann et al.[35] by means of LDA measurement. The advantage of LES approach over RANS was shown by the comparison between the numerical prediction and the LDA measurement. Min and Gao[36] investigated the mixing process in a stirred tank with a 3-narrow blade hydrofoil CBY impeller by means of LES and RANS approaches. The LES approach was found to achieve better accuracy than RANS for the calculation of power demand and mixing time.

The present study investigates the fluid flow instabilities in a baffled, stirred tank generated by a single Rushton turbine by means of LES. The sliding mesh method was used for the coupling between the rotating and the stationary frame of reference. The results from the LES simulations were investigated with a focus on velocity fluctuations and instantaneous circulation patterns of the fluid flow in the stirred tank. The fluctuations of radial and axial velocity were investigated for the monitoring points distributed over the vertical cross section of the tank. Flow circulation patterns in the three vertical sections of the tank were examined for different time instants. Vortices and their developments were also investigated based on the LES predicted instantaneous velocity fields. Simulations using the k-ε turbulent model were carried out on the same tank as a comparison. The flow fields predicted by the LES simulation and the simulation using standard the k-ε model were compared to the results from PIV measurement. All the simulations were conducted using CFD code CFX 5.

2 STIRRED TANK CONFIGURATION AND PIV MEASUREMENT

The stirred tank used in this research is a cylindrical Plexiglas tank. The tank, with a diameter (T) of 0.28 m, is equipped with four baffles (width $W=T/10$, 90° apart) and is filled with water up to $H=T$. A four-blade Rushton turbine impeller (diameter $D=T/2$, blade height $b=D/5$, blade width $a=D/4$) was used to generate liquid flow. The impeller clearance, C, is fixed at $T/2$. The configuration of the tank and the impeller is shown in Fig. 1.

Liquid flow in the stirred tank was investigated by means of PIV measurement and FlowMap 1500 system from Dantec Dynamics was used. The tank was seeded with polyamide seeding particles from Dantec. The diameter of the polyamide particles is approximately 20 μm diameter and the density of the particles is 1030 $kg \cdot m^{-3}$. An up to 20 Hz pulsed Nd:Yag laser with a beam expanding lens was used to illuminate the measurement area. A light sheet of 10 mm thickness was created at a vertical plane in the tank. A Nikon Hisence CCD camera was placed at the right angle to the light sheet to record images with a resolution of 1280×640 pixels. The recorded images were divided into an interrogation area of 64×64 pixels with 50% overlap, resulting in approximately 660 velocity vectors for the plane.

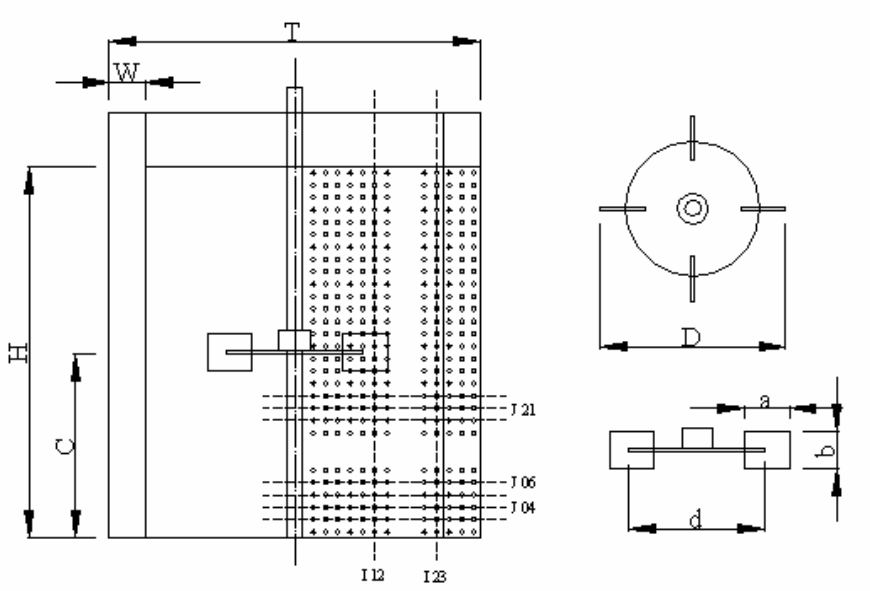

Figure 1 Stirred tank configuration, impeller geometry and location of the experimental points with a mesh size of 4.7 mm×4.7 mm in the PIV measurement

Based on the nearly instantaneous velocity field obtained from the PIV measurement, the time averaged velocity field was calculated as

$$\overline{u_{i,j}} = \frac{1}{N}\sum_{n=1}^{N} u_{i,j,n} \qquad \overline{v_{i,j}} = \frac{1}{N}\sum_{n=1}^{N} v_{i,j,n} \tag{1}$$

where u, v denote radial and axial velocity components respectively, i and j denote position in radial and axial direction; n denotes the nth flow field in the time series and N is the total number of flow field obtained. The time-averaged velocity field was compared to the result from the LES simulation and the simulation using k-ε turbulent model.

3 LARGE EDDY SIMULATION

In the LES approach, the governing equations are obtained by spatially filtering the Navier-Stokes equations. The large turbulent scales are computed explicitly, while the small scales are modeled using one available subgrid-scale (SGS) models, which describe interactions between the resolved and unresolved scales.

Filtering eliminates eddies whose scales are smaller than the filter width. In the current study, a top-hat filter with the filter width to grid size ratio being two is used. Applying the filtering operation to the momentum equation leads to

$$\frac{\partial \overline{\rho}\widetilde{u}_i}{\partial t} + \frac{\partial \overline{\rho}\widetilde{u}_i\widetilde{u}_j}{\partial x_j} = -\frac{\partial \overline{p}}{\partial x_i} + \frac{\partial \overline{\tau_{ij}}}{\partial x_j} + \frac{\partial \overline{\sigma_{ij}}}{\partial x_j} \tag{2}$$

where τ_{ij} is the filtered stress tensor, σ_{ij} is SGS stresses, which has the following definition:

$$\sigma_{ij} = -\left(\overline{\rho u_i u_j} - \overline{\rho}\widetilde{u}_i\widetilde{u}_j\right) \tag{3}$$

These SGS stresses are unknown, and need to be modeled. Smagorinsky[37] developed the most basic subgrid scale model, in which the turbulent viscosity is modeled by

$$\mu_t = \rho L_s^2 \left|\overline{S}\right| \tag{4}$$

$$\left|\overline{S}\right| = \sqrt{2\overline{S_{ij}}\,\overline{S_{ij}}} \qquad \overline{S_{ij}} = \frac{1}{2}\left(\partial_j \overline{u_i} + \partial_i \overline{u_j}\right) \tag{5}$$

where L_s is the mixing length of subgrid scales, defined as

$$L_s = \min\left(k \cdot d \cdot C_s \cdot V^{1/3}\right) \tag{6}$$

where k is the von Kármán constant, d is the distance to the closest wall, and V is the volume of the computational cell, and C_s has a constant value of 0.1.

The computational model of the tank contains a full three dimensional (360°) grid with a total of 477,160 unstructured, non-uniformly distributed, hexahedral cells. The grid statistics is presented in Table 1. A finer grid with 183,560 cells was created in the impeller region, while a coarser grid with 293,600 cells was used in the bulk region of the tank. In the impeller region, the maximum cell volume is 21.9 mm^3 and the minimum cell volume is 1.32 mm^3, while in the bulk region, the maximum cell volume and the minimum cell volume are 83.9 mm^3 and 4.78 mm^3 respectively. If the grid cells were cubes, this would represent a maximum resolved grid length of 2.8 mm and a minimum of 1.1 mm for the impeller region and a maximum of 4.38 mm and a minimum of 1.68 mm for the bulk region. The resolved scale is much larger than the Kolmogorov scale (0.1 mm) but much smaller that the large scale flow motions of interest (0.1 m), therefore fulfills the grid density requirement of LES approach.

The discretized equations were solved using an algebraic multigrid procedure. A central differencing scheme was used for spatial discretization of the momentum equations and a second-order implicit scheme was used for time advancement in the simulation. Implicit time steps in the range of 0.0167-0.0667 s were used. The transient impeller motion was modeled using the sliding mesh method for unstructured grids. The simulations were conducted by means of the parallel version of CFX on a supercomputer “ShenCao 21C”, which has 128 dual processors and a maximum frequency of 1500 Gflops.

Table 1 The statistics of grid cells in the impeller and the bulk region

Impeller region	cell number (-)	183560
	maximum cell volume, mm^3	21.9
	minimum cell volume, mm^3	1.32
	maximum grid length, mm	2.8
	minimum grid length, mm	1.1
Bulk region	cell number (-)	293600
	maximum cell volume, mm^3	83.9
	minimum cell volume, mm^3	4.78
	maximum grid length, mm	4.38
	minimum grid length, mm	1.68

4 RESULT AND DISCUSSION

4.1 Velocity fluctuations

The LES simulation was carried out with quiescent liquid as a start and for approx. 3900 time steps with 0.0667 s per time step. The simulation using the standard k-ε model started from the beginning with a time step of 2 s. After 20 time steps, the simulation was continued with the time step of 0.0667 s. From this instant on, the axial and radial velocities at points on the vertical cut plane in the tank were monitored. The simulation was completed after approx. 3300 time steps, i.e. 260 s. The location of the monitor points is illustrated in Fig. 2. Figure 3 presents the axial and radial velocities versus time steps in the simulation using the k-ε model and Fig. 4 presents velocity fluctuations in the LES simulation.

From Fig. 3, it can be seen that the axial and radial velocities are varying with time and that the velocities in the bulk region reach stabilized state faster than those in the impeller region. In the bulk region, the axial and radial velocities become stabilized when the simulation time is greater than 50 s while in the impeller region, the velocities do not reach a stabilized state until the simulation time is greater than 60 s. Periodical fluctuations of the radial and axial velocities are observed in the impeller region and in the jet flow coming off the impeller blades, which is due to the effect of the blade passages. It should be noted that for clarity of the figure the axial and radial velocity were sampled at a constant interval so only values of a part of the time steps were shown. It is not shown in the figure that the frequency of the velocity fluctuations is 2 Hz, corresponding to the frequency of the blade passages. Weaker periodical velocity fluctuations were observed in the bulk region of the tank.

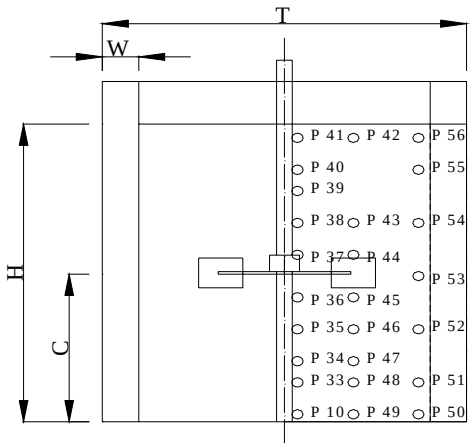

Figure 2 Location of the monitor points in CFD simulation

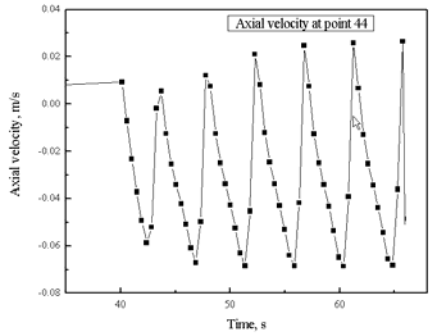

(a) Axial velocity in the impeller region

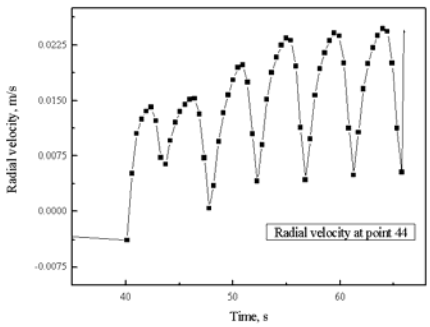

(b) Radial velocity in the impeller region

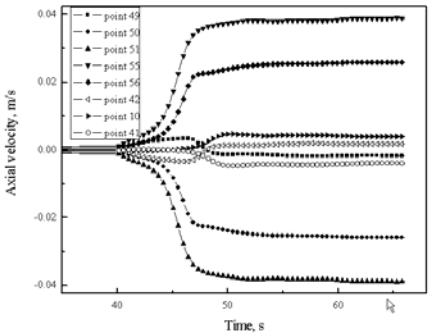

(c) Axial velocity in the bulk region

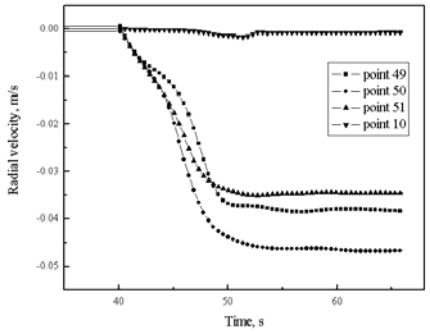

(d) Radial velocity in the bulk region

Figure 3 Velocity versus time steps in the simulation using standard k-ε model (N_I＝30 rpm, water, Re＝9720, k-ε model, tank diameter 282 mm)

As shown in Fig. 4, the fluctuations of axial and radial velocities (black line) predicted by the LES simulation are quite stochastic and complex, with high and low frequencies fluctuations. In the impeller region (point 45), velocity fluctuations of high frequencies are observed, while velocity fluctuations of low frequencies are observed in the bulk flow. The grey line shows the smoothed axial and radial velocities with high frequencies fluctuations filtered out by FFT. A periodical velocity fluctuation with approximately the period of 75 s can be seen in the time series of the smoothed velocities at both points 45 and 55. The periodical fluctuation corresponds to a nondimensional MI frequency of 0.027. The nondimensional MI frequency is defined as the ratio of MI frequency (0.013 Hz) to impeller rotational speed (0.5 Hz). This result agrees with the findings of Galletti et al.[14] and Nikiforaki et al.[11], who investigated MI frequencies by means of LDA measurements. According to their findings, at a Re number of 9720, there are MIs with 2 frequency bands present. For the lower frequency band MI, they found that the dependence of the MI frequency on the impeller rotational speed is linear with a proportional constant of approximately 0.02. The MI found in this study belongs to the lower frequency band MI. However, FFT and spectra analysis of the LES predicted velocity series are necessary in future work to gain more understandings to the complicated flow instabilities.

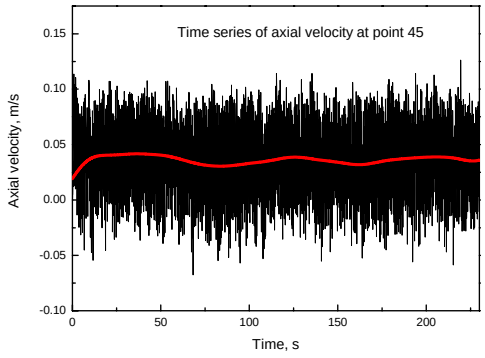

(a) Axial velocity in the impeller region

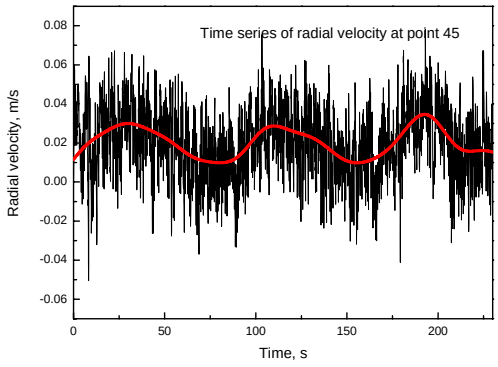

(b) Radial velocity in the impeller region

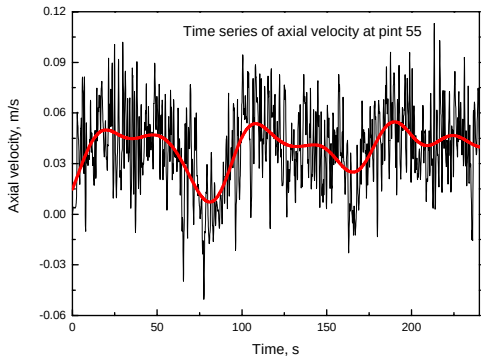

(c) Axial velocity in the bulk region

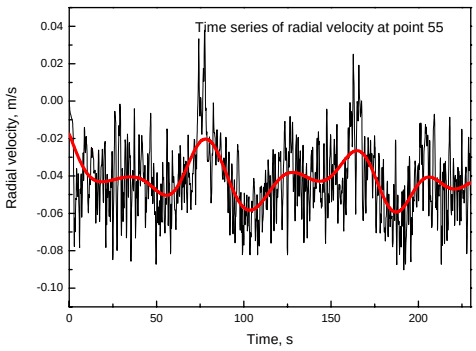

(d) Radial velocity in the bulk region

Figure 4 Velocity fluctuations with time in the simulation using LES approach (N_I＝30 rpm, water, *Re*＝9720, LES model, tank diameter 282 mm)

4.2 Flow circulation patterns

Historically, the flow circulation pattern in a Ruston turbine agitated tank was thought to be symmetric. The jet flow coming off the impeller blades streams towards the wall and divides into two flows under the influence of the vessel wall: one downward along the wall, to the bottom of the vessel, then back to the impeller region; the other rise along the wall, to the top of the vessel and back to the impeller region, forming an symmetric double loop. In contrast to this simple picture, flow fields in the tank are rather complex and unstable. These unstable flow phenomena in the vessel were identified as macro-instabilities (MI)[7,8,11-14].

The flow pattern predicted by the simulation using the *k*-*ε* model is shown in Fig. 5. From the velocity field (in the view plane 0-180°), the symmetry of liquid flow can be apparently seen between the right and the left part of tank, and between the upper and the lower part of the tank. In reality, this is not the case. Liquid flows in stirred tanks are transient, rather complex and asymmetric.

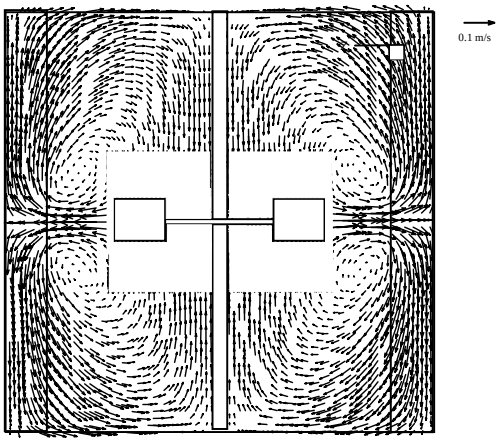

Figure 5 Velocity field obtained using the standard k-ε model (N_I = 30 rpm, water, tank diameter 282 mm)

The advantage of LES approach over the k-ε model is its capability to fully resolve the large turbulent scales, which makes LES approach a computationally feasible means to investigate the time-varying characteristics of the flow in stirred tank. Figure 6 shows the instantaneous circulation patterns produced by the Ruston turbine. Figures 6(a), 6(d), 6(g), Figs. 6(b), 6(e), 6(h) and Figs. 6(c), 6(f), 6(i) are the results for the plane 0-180°, 45-225° and 90-270° respectively. The position of those view planes seen from the top is schematically shown in Fig. 7.

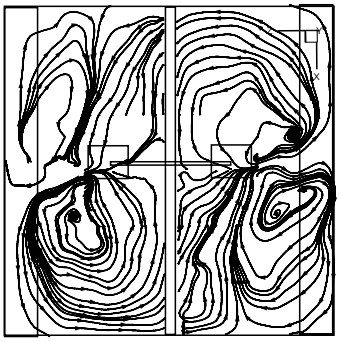

(a) t=240.12 s, 0°-180°

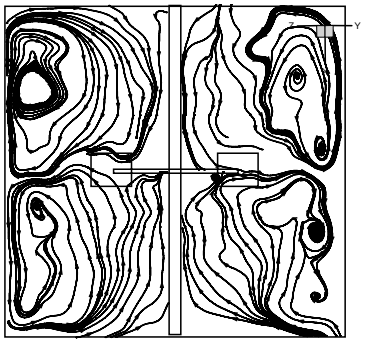

(b) 45°-225°

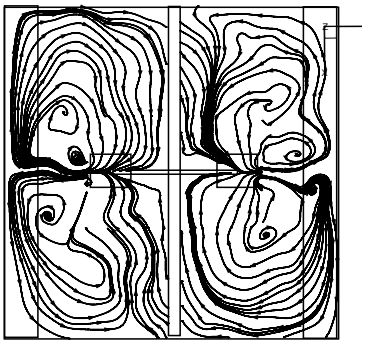

(c) 90°-270°

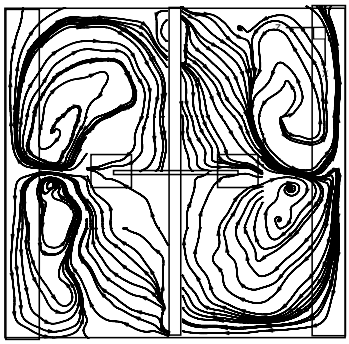

(d) t=256.68 s, 0°-180°

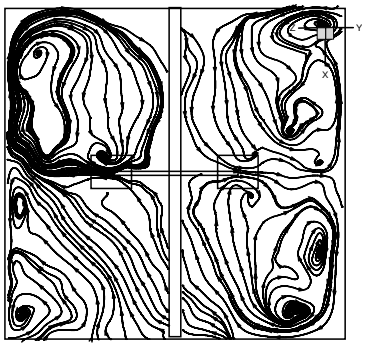

(e) 45°-225°

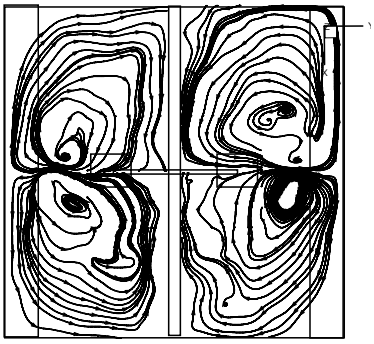

(f) 90°-270°

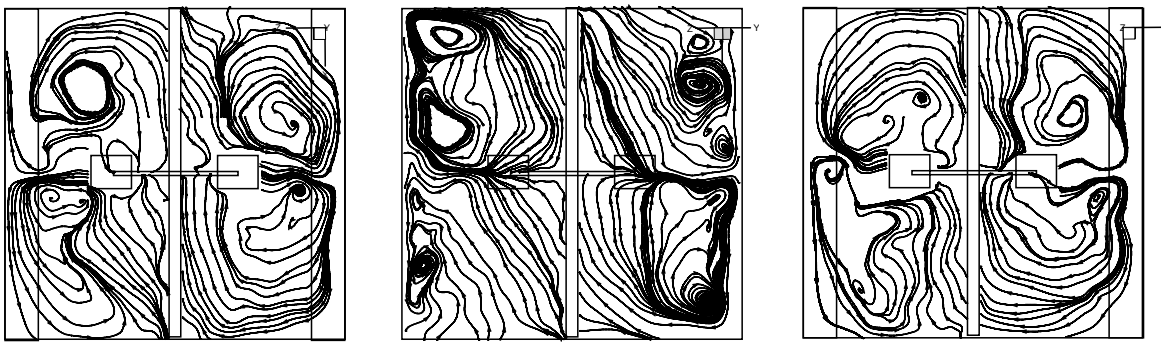

(g) t=260.00 s, 0°-180° (h) 45°-225° (i) 90°-270°

Figure 6 Instantaneous flow circulation patterns predicted by the LES simulation (N_I＝30 rpm, water, Re＝9720, LES model, tank diameter 282 mm)

From the instantaneous flow fields provided by the LES simulation, large-scale asymmetric liquid flow is found to span a large portion of the tank. From Fig. 6(a), one stream transverses axis from the right to the left at the top of the tank while at the bottom of the tank another stream passes the axis from the left to the right forming an overall counter-clockwise flow circulation in the vertical plane. For different view planes (45-225°, 90-270°) the circulation patterns are different.

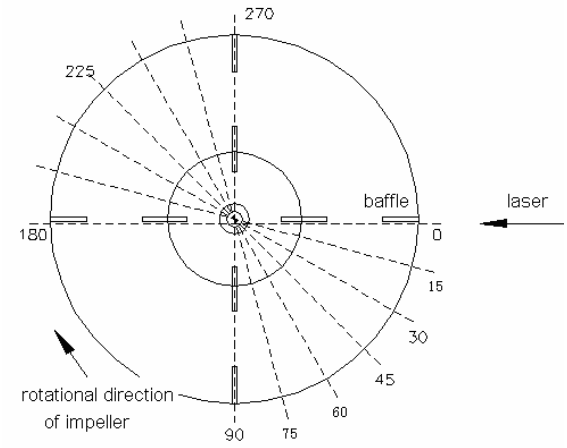

Figure 7 Schematic illustration of the view planes

From Figs. 6(b), 6(e), 6(h), and Figs. 6(c),6 (f), 6(i), it can be seen that these asymmetric flow patterns change from one plane to another and from time to time. The overall flow pattern at the view plane 0-180° becomes clockwise at t=256.68 s. Similar unstable and asymmetric flow circulation patterns dominating the entire tank are observed by Roussinova et al.[12] in the instantaneous velocity field produced by a 45° PBT. From these instantaneous flow fields provided by the LES simulation, it is indicated that fluid flow in the stirred tank is asymmetric, stochastic and complex with large-scale vortices. These time-varying large-scale vortices dominate the entire tank and have great influence on the mixing process in the tank.

4.3 Instantaneous velocity fields

The vortices and their development in the stirred tank were investigated using a short time step of 0.0167 s. The calculation was carried out based on the result flow field at t=401.58 s (after 6020 iterations). Figure 8 shows the instantaneous velocity fields in the view plane 0-180° at two time instants separated by 1.58 s, which corresponds to approximately three times a blade passage period.

In Fig. 8(a) there are many vortices at different scales, of which three vortices (A, B, C) can be clearly observed. Vortices A and B develop near the tip of the impeller blade in the left and the right part of the tank respectively. Vortex C forms in the corner where the vessel wall meets the liquid surface. After 95 time steps (with a time step of about 0.0167s), Fig. 8(b) is obtained. It can be seen that vortex A coming from the blade has moved radially outwards and then downwards along the wall, while vortex B has moved upwards along the wall with a relatively lower moving speed. At the left top corner of the tank, vortex C has disappeared, while vortex D appears. At the right part of the tank near the tank corner, vortex E and vortex F appear. Fluid flow in a stirred tank is asymmetric and fluctuating, with vortices of different scales stochastically appearing, developing and disappearing in the entire tank for all time.

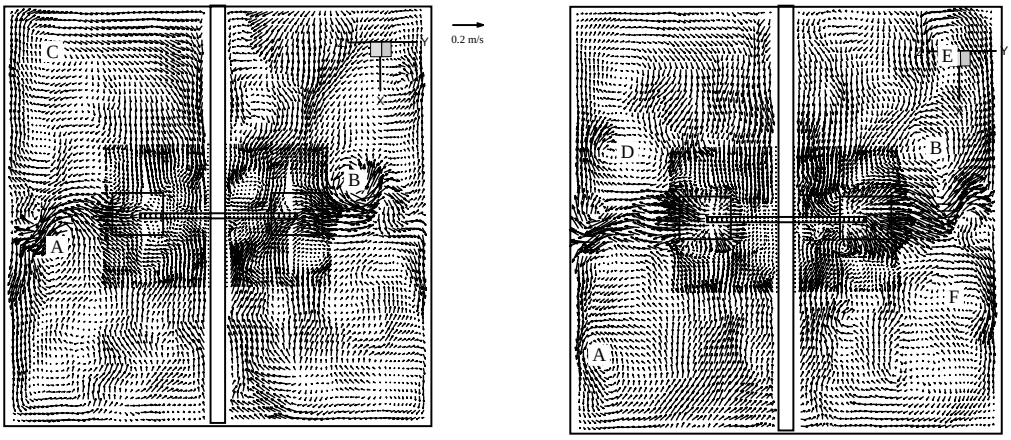

(a) t=401.58 s (b) t=403.16 s

Figure 8 Development of vortices shown by the LES simulation (N_I=30rpm, water, LES model, tank diameter 282 mm)

4.4 Comparison with PIV measurement

The flow fields predicted by LES and the standard k-ε model were compared to the PIV measurement. Figure 9 presents the comparison of velocity fields obtained by the PIV measurement and by the LES simulation. Figure 9(a) shows the velocity fields from the PIV measurement, which is obtained by averaging 1024 semi-instantaneous velocity fields. Detailed information on the PIV measurement can be found in the previous work[13]. The whole velocity field is constructed by means of mirror since only velocity for the right part of the tank is available from the measurement.

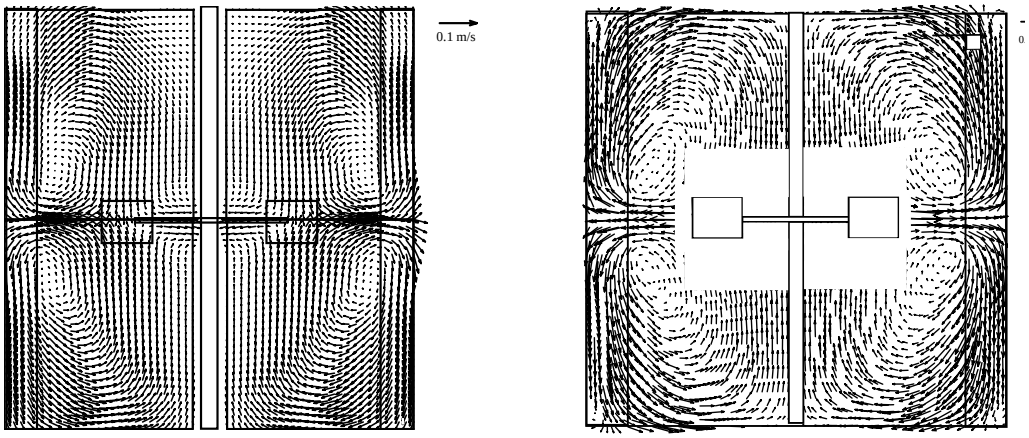

(a) PIV measurement (b) LES simulation

Figure 9 Comparison between time-averaged velocity fields obtained from PIV measurement and from the LES simulation (N_I＝30 rpm, water, tank diameter 282 mm)

Figure 9(b) presents the averaged velocity field from LES simulation, which is an average of 3000 instantaneous velocity fields. Results show that the time averaged velocity field cannot be accurately obtained if the overall number of the instantaneous velocity fields is less than 500. When the number of the overall velocity fields is greater than 2000, the time averaged values tend to be stable.

When we compare Figs. 5 and 9, good agreement can be seen between the simulation using the standard k-ε model, the LES simulation and the PIV measurement. Figure 10 gives quantitative comparison between the simulations and the measurement. For both the LES approach and the simulation using the k-ε model, the accuracy of prediction of radial velocities is better than that of the axial velocities. The simulation using the k-ε model is almost as accurate as the LES approach for the prediction of radial velocity, however worse than the LES simulation for the prediction of axial velocities.

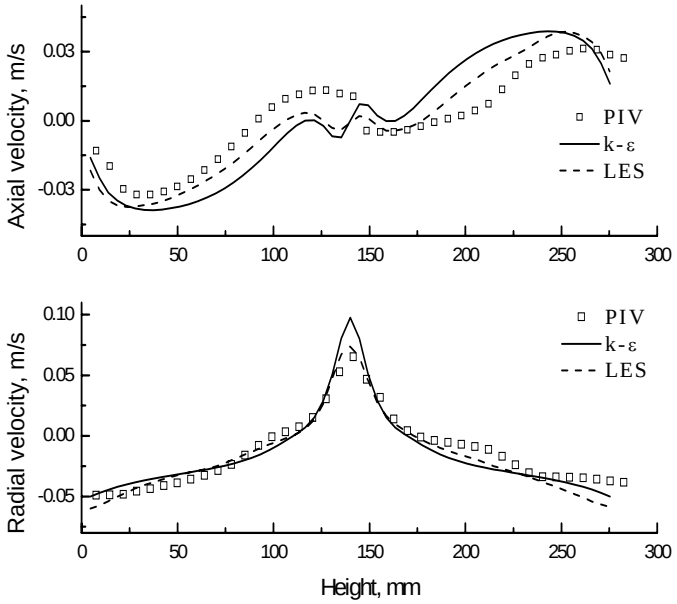

Figure 10 Comparison of velocities at radial distance of 0.1 m at the plane of baffle (N_I＝30 rpm, water, Re＝9720, tank diameter 282 mm)

5 CONCLUSION

The flow instabilities in a baffled, stirred tank generated by a single Rushton turbine is investigated by means of large eddy simulation (LES). The sliding mesh method is used for the coupling between the rotating and the stationary frame of references. The flow fields predicted by the LES and the standard k-ε model are compared to results from the PIV measurement.

Results show that there is good agreement between the simulations using the k-ε model, the LES simulations and the PIV measurements. The accuracy of prediction of radial velocities is better than that of the axial velocities for both the LES simulations and the simulations using the k-ε model. For the prediction of axial velocity, the LES approach is better than the standard k-ε model. The LES simulation predicts fluctuations of the radial and axial velocity at different frequencies.

Velocity fluctuations of high frequencies are observed in the impeller region, while velocity fluctuations of low frequencies are observed in the bulk flow. A periodical fluctuation with a nondimensional frequency of 0.027 can be seen in the axial and radial velocity series, which agrees with experimental investigations in the literature. However, FFT and spectra analysis of the LES calculated velocity series are necessary in future work to gain deep understandings of the complicated flow instabilities. Circulation patterns predicted by LES are asymmetric, stochastic and complex, spanning a large portion of the tanks and varying with time, while circulation patterns obtained by the k-ε simulations are symmetric.

NOMENCLATURE

a	blade width, m	ρ	fluid density, kg·m^{-3}
b	blade height, m	$\overline{p}$	filtered pressure field, kg·m^{-1}·s^{-2}
C	clearance, m	τ_{ij}	filtered turbulent stress tensor, kg·m^{-1}·s^{-2}
D	impeller diameter, m	σ_{ij}	SGS stress tensor, kg·m^{-1}·s^{-2}
H	liquid height in reactor, m	μ_t	turbulent viscosity, m^2·s^{-1}
i, j	index, dimensionless	Abbreviation	
L_s	subgrid scale mixing length, m	CCD	charge couple device
n	flow field number in the time series, dimensionless	CFD	computational fluid dynamics
N	total number of flow fields, dimensionless	DNS	direct numerical simulation
N_I	impeller Rotational speed, s^{-1}	LDV/LDA	laser Doppler velocimetry/ laser Doppler anemometry
Re	impeller Reynolds number, dimensionless, $N_I D^2/v$	LES	large eddy simulation
$\lvert\overline{S}\rvert$	characteristic filtered rate of strain ($\lvert\overline{S}\rvert = \sqrt{2\overline{S_{ij}}\,\overline{S_{ij}}}$)	MI	macro-instability
$\overline{S_{ij}}$	filtered rate of strain ($\overline{S_{ij}} = \frac{1}{2}(\partial_j \overline{u_i} + \partial_i \overline{u_j})$)	PBT	pitched blade turbine
T	reactor diameter, m	PIV	particle image velocimetry
t	time step, s	POD	proper orthogonal decomposition
$\widetilde{u}$	filtered velocity component, m·s^{-1}	PSD	power spectral density
$u_{i,j,n}$ $v_{i,j,n}$	nth instantaneous velocity in the radial and axial direction respectively, m·s^{-1}	RANS	Reynolds averaged Navier-Stokes
W	baffle width, m	RT	Rushton turbine

REFERENCES

1. Van't Riet, K., Bruijn, W., Smith, J.M., "Real and pseudo-turbulence in the discharge stream from a Rushton turbine", *Chem. Eng. Sci.*, **31**(6), 407-412 (1976).
2. Ranade, V.V., Joshi, J.B., "Flow generated by a disc turbine: Part I experimental", *Trans. IChemE*, **68**A, 19-32 (1990).
3. Schaefer, M., Hoefken, M., Durst, F., "Detailed LDV measurements for visualization of the flow field within a stirred tank reactor equipped with a Rushton turbine", *Trans. IChemE*, **75A**, 729-736 (1997).

4. Lee K. C., Yianneskis M., “Turbulence properties of the impeller stream of a Rushton turbine”, *AIChE J.*, 44, 13-24(1998).
5. Ranade, V.V., Perrard, M., Sauze, N.L. Xuereb C., Bertrand J., “Trailing vortices of Rushton turbine: PIV measurement and CFD simulation with snapshot approach”, *Trans. IChemE*, **79A**, 3-11 (2001).
6. Sharp, K.V., Adrian, R.J., “PIV study of small scale flow structure around a Rushton impeller turbine”, *AIChE J.*, **47**(4), 766-778 (2001).
7. Myers, K.J., Ward, R.W., Bakker, A., “A digital particle image velocimetry investigation of flow field instabilities of axial flow impeller”, *J. Fluids Eng.*, **119**, 623- 632 (1997).
8. Montes, J.L., Boisson, H.C., Fort, I., Jahoda, M., “Velocity field macro-instabilities in an axially agitated mixing vessel”, *Chem. Eng. J.*, **67**, 139-145 (1997).
9. Hasal, P., Montes, J.L., Boisson, H.C., Fort, I., “Macro-instabilities of velocity field in stirred vessel: detection and analysis”, *Chem. Eng. Sci.*, **55**, 391-401 (2000).
10. Roussinova, V.T., Grgic, B., Kresta, S.M., “Study of macro-instabilities in stirred tanks using a velocity decomposition technique”, *Trans. IChemE*, **78A**, 1040-1052 (2000).
11. Nikiforaki, L., Montante, G., Lee, K.C., Yianneskis, M., “On the origin, frequency and magnitude of macro-instabilities of the flows in stirred vessels”, *Chem. Eng. Sci.*, **58**, 2937-2949 (2003).
12. Roussinova, V., Kresta, S.M., Weetman, R., “Low frequency macroinstabilities in a stirred tank: scale-up and prediction based on large eddy simulations”, *Chem. Eng. Sci.*, **58**, 2297-2311 (2003).
13. Fan, J.H., Rao, Q., Wang, Y.D., Fei, W.Y., “Spatio-temporal analysis of macro-instability in a stirred vessel via digital particle image velocimetry (DPIV)”, *Chem. Eng. Sci.*, **59**, 1863-1873 (2004).
14. Galletti, C., Paglianti, A., Lee, K.C., Yianneskis, M., “Reynolds number and impeller diameter effects on instabilities in stirred vessels”, *AIChE J.*, **50**(9), 2050-2063 (2004).
15. Harvey, P.S., Greaves, M., “Tuebulent flow in an agitated vessel, Part I: A predictive model”, *Trans IChemE*, **60**, 195-210 (1982).
16. Brucato, A., Ciofalo, M., Grisafi, F., Rizzuti L., “Computer simulation of turbulent fluid flow in baffled and unbaffled tanks stirred by radial impellers”, V.G. Dovi eds., *Proceedings of International Conference of Computer Applications to Batch Processes*, Cengio, Italy, 69-86 (1990).
17. Fokema, M.D., Kresta, S.M., Wood, P.E., “Importance of using the correct impeller boundary conditions for CFD simulations of stirred tanks”, *Can. J. Chem. Eng.*, **72**, 177-183 (1994).
18. Xu, Y., McGrath, G., “CFD predictions of stirred tank flows”, *Trans. IChemE*, **74A**, 471-475 (1996).
19. Takeda, H., Narasaki, K., Kitajima, H., Sudoh S., Onofusa M., Iguchi S., “Numerical simulation of mixing flows in agitated vessels with impellers and baffles”, *Comput. Fluids*, **22**(2/3), 223-228 (1993).

20. Luo, J.Y., Gosman, A.D., Issa, R.I., Middleton J.C., Fitzgerald M.K. “Full flow field computation of mixing in baffled stirred vessels”, *Trans. IChemE*, **71A**, 342-344 (1993).
21. Luo, J.Y., Issa, R.I., Gosman, A.D., “Prediction of impeller-induced flows in mixing vessels using multiple frames of reference”, *IChemE Symp. Ser.*, **136**, 549-556 (1994).
22. Ranade, V.V., Dommeti, S., “Computational snapshot of flow generated by axial impellers in baffled stirred vessels”, *Trans. IChemE*, **74**, 476-484 (1996).
23. Brucato, A., Grisafi, F., Micale, G., “Numerical prediction of flow fields in baffled stirred vessels: A comparison of alternative modeling approaches”, *Chem. Eng. Sci.*, **53**(21), 3653-3684 (1998).
24. Jenne, M., Reuss, M., “A critical assessment on the use of k-ε turbulence models for simulation of the turbulent liquid flow induced by a Rushton turbine in baffled stirred tank reactors”, *Chem. Eng. Sci.*, **54**, 3921-3939(1999).
25. Sun, H.Y., Wang, W.J., Mao, Z.-S., “Numerical simulation of the whole three dimensional flow in a stirred tank with anisotropic algebraic stress model”, *Chinese J. Chem. Eng.*, **10**(1), 15-24 (2002).
26. Fan, L., Wang, W.J., Yang, C., Mao, Z.-S., “Numerical simulation of laminar flow field in a stirred tank”, *Chin. J. Chem. Eng.*, **12**(3), 324-329 (2004).
27. Min, J., Gao, Z.M., Shi, L.T., “CFD simulation of mixing in a stirred tank with multiple hydrofoil impellers”, *Chin. J. Chem. Eng.*, **13**(5), 583-588 (2005).
28. Bartels, C., Breuer, M., Wechsler, K., Durst, F., “Computational fluid dynamics applications on parallel-vector computers: computation of stirred vessel flows”, *Comput. Fluids*, **30**(1), 69-97 (2001).
29. Eggels, J.G.M., “Direct and large-eddy simulations of turbulent fluid flow using the lattice-boltzmann scheme”, *Int. J. Heat Fluid Flow*, **17**(3), 307-323 (1996).
30. Derksen, J., van den Akker, H.E.A., “Large eddy simulation on the flow driven by a Rushton turbine”, *AIChE*, **45**(2), 209-221 (1999).
31. Derksen, J., “Assessment of large eddy simulations for agitated flows”, *Trans IChemE*, **79A**, 824-830 (2001).
32. Revstedt, J., Fuchs, L., Tragardh, C., “Large eddy simulations of the turbulent flow in a stirred reactor”, *Chem. Eng. Sci.*, **53**(24), 4041-4053 (1998).
33. Bakker, A., Oshinowo, L.M., Marshall, E.M., “The use of large eddy simulation to study stirred vessel hydrodynamics”, *Proceedings of 10th European Conference on Mixing*, Amsterdam, Elsevier Science, 247-254 (2000).
34. Alcamo, R., Micale, G., Grisafi, F., Brucato A., Ciofalo M., “Large-eddy simulation of turbulent flow in an unbaffled stirred tank driven by a Rushton turbine”, *Chem. Eng. Sci.*, **60**, 2303-2316 (2005).
35. Hartmann, H., Derksen, J., Montavon, C., Pearson J. Hamill I.S., van den Akker H.E.A., “Assessment of large eddy and RANS stirred tank simulations by means of LDA”, *Chem. Eng. Sci.*, **59**, 2419-2432 (2004).

36. Min, J., Gao, Z.M., “Large eddy simulations of mixing time in a stirred tank”, *Chin. J. Chem. Eng.*, **14**(1), 1-7 (2006).
37. Smagorinsky, J., “General circulation experiments with the primitive equations, I. The Basic Experiment”, *Moth. Wea. Rev.*, **91**, 99-164 (1963).